Supporting Information

Synthesis of a 6-Methyl-7-Deaza Analogue of Adenosine that Potently Inhibits Replication of Polio and Dengue Viruses

Runzhi Wu, Eric D. Smidansky, HyungSuk OH, RatreeTakhampunya, Radhakrishnan Padmanabhan, Craig E. Cameron, and Blake R. Peterson*

Department of Medicinal Chemistry, The University of Kansas, Lawrence, KS 66047, Department of Biochemistry and Molecular Biology, The Pennsylvania State University, University Park, PA 16802, and Department of Microbiology and Immunology, Georgetown University School of Medicine, Washington DC 20057

Table of Contents

Analysis of compound purity by analytical HPLC

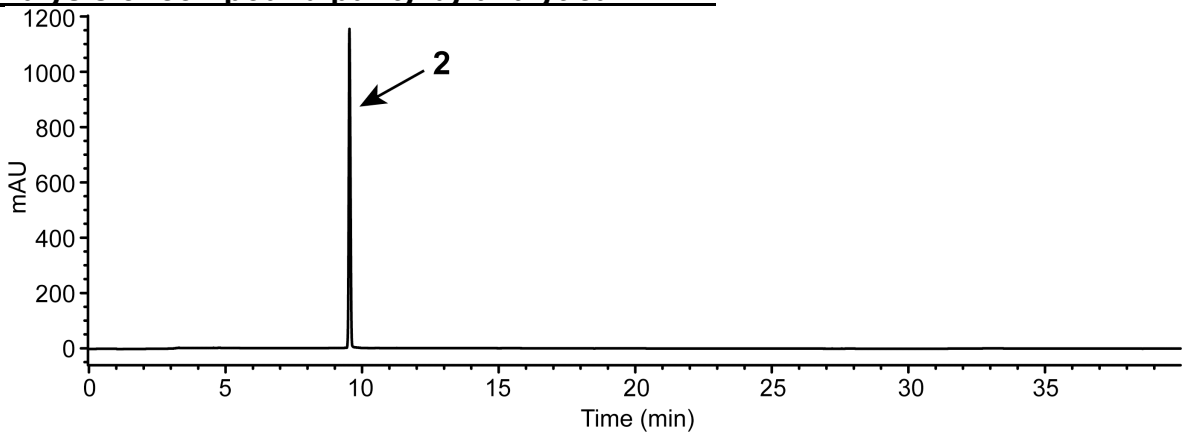

Figure S1. Analytical reverse-phase HPLC profile of 6-methyl-9-β-D-ribofuranosylpurine(**2**) after recrystallization. Retention time = 9.5 min. Purity = 98 %. Absorbance wavelength = 254 nm.

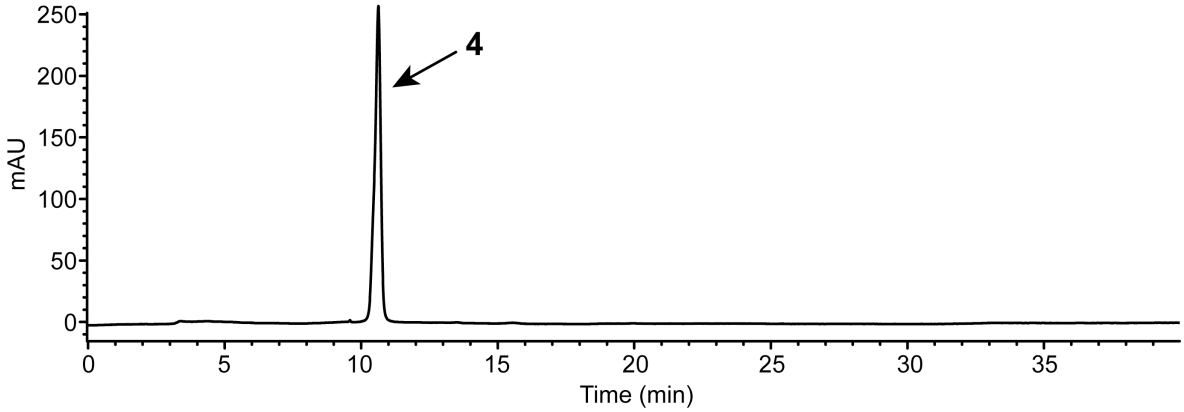

Figure S2. Analytical reverse-phase HPLC profile of 7-methyl-3-β-D-ribofuranosyl-3*H*-imidazo[4,5-*b*]pyridine (1-deaza-6-methyl-9-β-D-ribofuranosylpurine, **4**) after recrystallization. Retention time = 10.6 min. Purity = 98%. Absorbance wavelength = 254 nm.

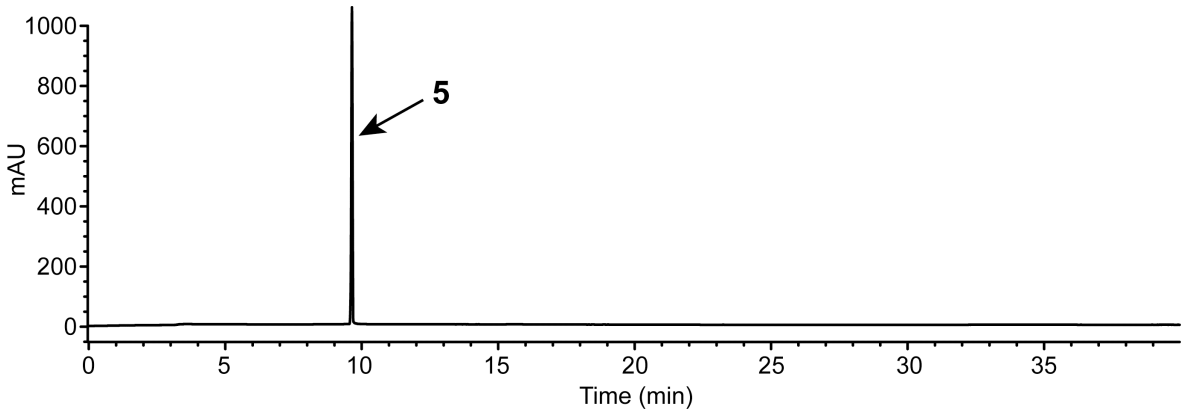

Figure S3. Analytical reverse-phase HPLC profile of 4-methyl-1-β-D-ribofuranosyl-1*H*-imidazo[4,5-*c*]pyridine (3-deaza-6-methyl-9-β-D-ribofuranosylpurine, **5**) after recrystallization. Retention time = 9.6 min. Purity = 99 %. Absorbance wavelength = 254 nm.

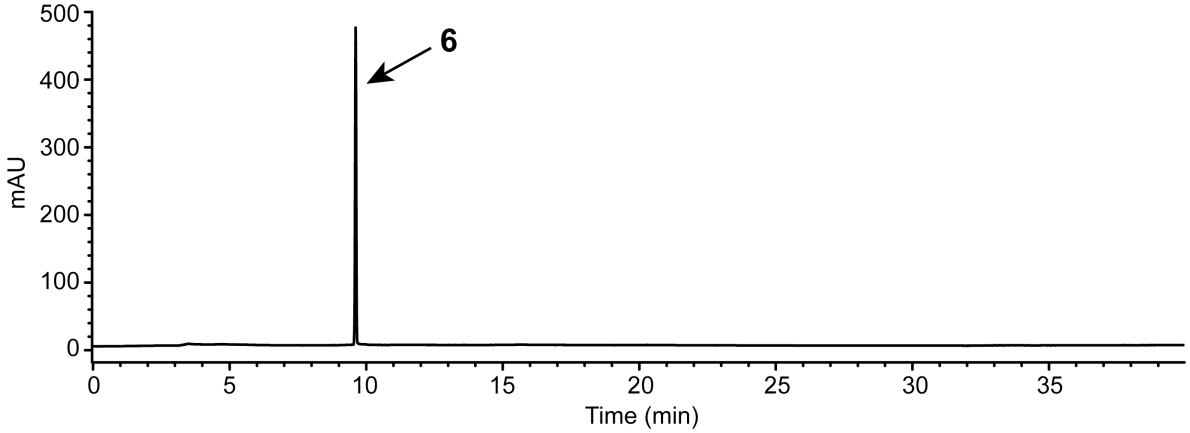

Figure S4. Analytical reverse-phase HPLC profile of4-methyl-7-β-D-ribofuranosylpyrrolo[2,3-*d*]pyrimidine (7-deaza-6-methyl-9-β-D-ribofuranosylpurine, **6**) after recrystallization. Retention time = 9.6 min. Purity = 98 %. Absorbance wavelength = 254 nm.

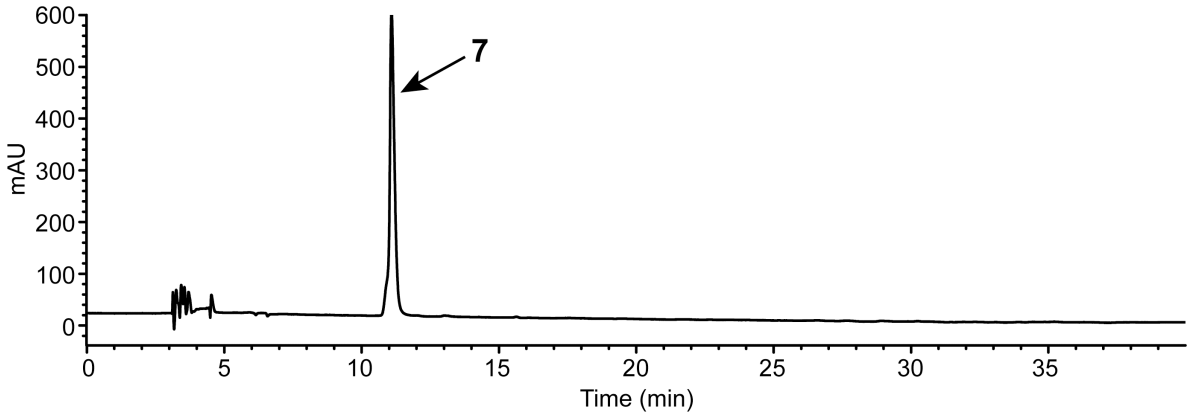

Figure S5. Analytical reverse-phase HPLC profile of 4-methyl-7-(5'-*O*-methyl-β-D-ribofuranosyl)pyrrolo[2,3-*d*]pyrimidine (7-deaza-6-methyl-9-(5'-*O*-methyl-β-D-ribofuranosyl)purine, **7**). Retention time = 11.1 min. Purity = 98 %. Absorbance wavelength = 254 nm.

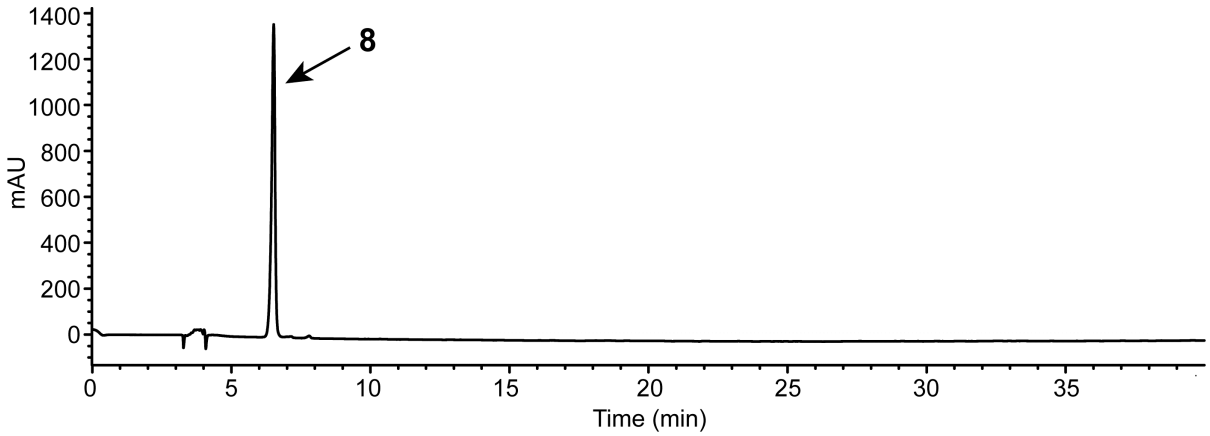

Figure S6. Analytical reverse-phase HPLC profile of 6-methyl-9-β-D-ribofuranosylpurine 5'-triphosphate (**8**). Retention time = 6.3 min. Purity = 98%. Absorbance wavelength = 254 nm.

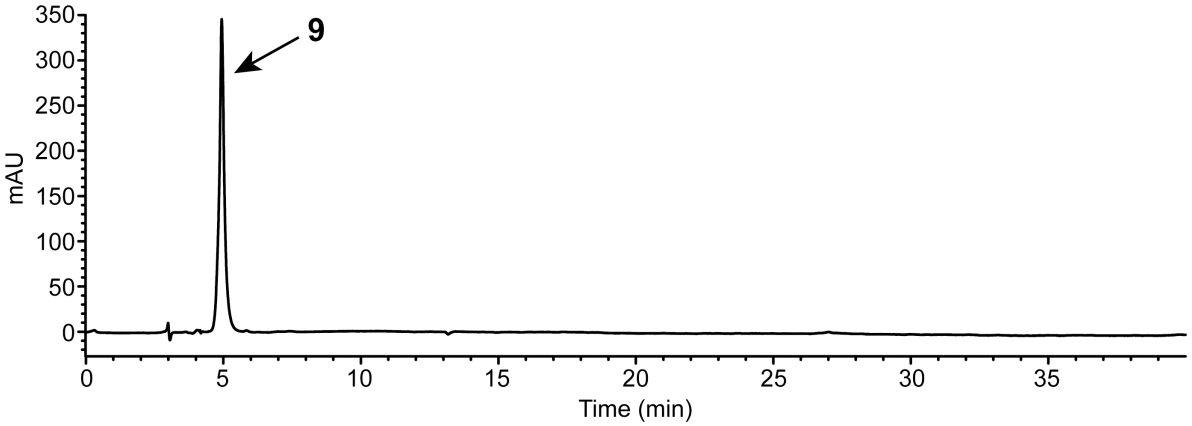

Figure S7. Analytical reverse-phase HPLC profile of 4-methyl-7-β-D-ribofuranosylpyrrolo[2,3-*d*]pyrimidine5'-triphosphate (7-deaza-6-methyl-9-β-D-ribofuranosylpurine 5'-triphosphate, **9**). Retention time = 4.9 min. Purity = 95 %. Absorbance wavelength = 254 nm.

Guanidine resistance assay data

Compound	Ribavirin	Ribavirin	**2**	**2**	**6**	**6**
Conc. (μM)	150	300	1.62	3.24	0.046	0.092
Gua^r plaques	150	>250	12	22	19	17

Table S1. Formation of guanidine-resistant plaques by **2**, **6** and ribavirin (a mutagenic control) in a guanidine resistance assay of viral mutagenesis.

NTP assay data

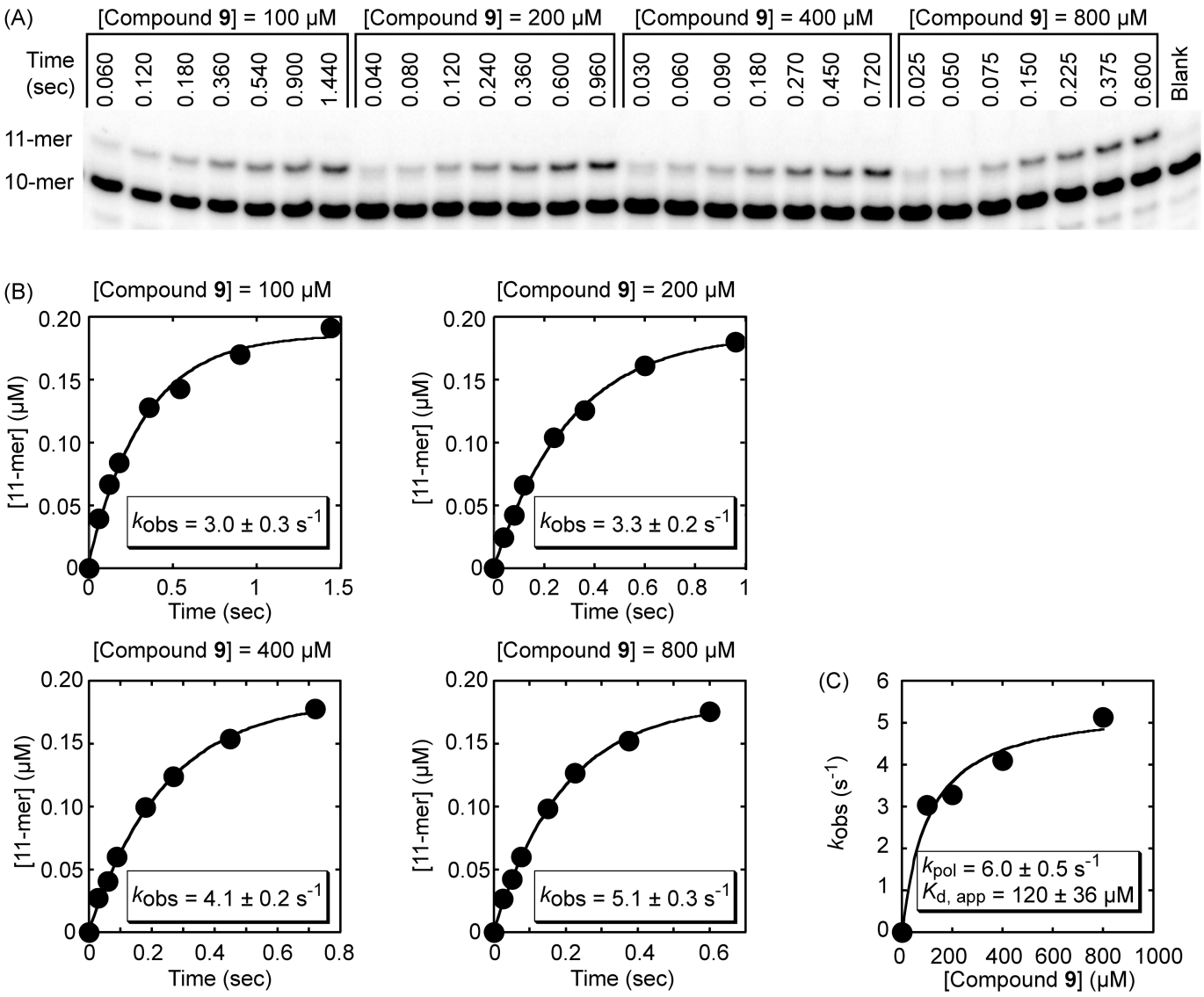

Figure S8. Panels A-C: Pre-steady state kinetics of incorporation of **9** into RNA opposite template U by PV RdRP. Panel A: Image of SDS PAGE gel of extended 10-mer ^{32}P-labeled RNA substrate (illustrated in Figure 3, Panel D) using 100, 200, 400 or 800 μM of **9**. Fast time points were taken using a chemical quench-flow rapid kinetics apparatus (KinTek Corp.). Panel B: Fits of 11-mer product formation as a function of time to a single exponential model, yielding observed rate constants, k_{obs}. Panel C: Replot of observed rate constants as a function of the concentration **9** and fit to a hyperbolic model yielding estimates of k_{pol}, the maximal rate constant for a single incorporation, and $K_{d,app}$, the kinetically-measured binding constant of **9** to the PV RdRP-RNA complex. Use of the chemical quench-flow apparatus to measure incorporation kinetics and fits to models were essentially as described in a reported procedure (*Biochemistry* **2004,** 43, 5126-5137). Note that compound **9** is fluorescent, preventing use of the stopped-flow apparatus to measure kinetics of incorporation, as was possible for non-fluorescent **8** (Figure S9).

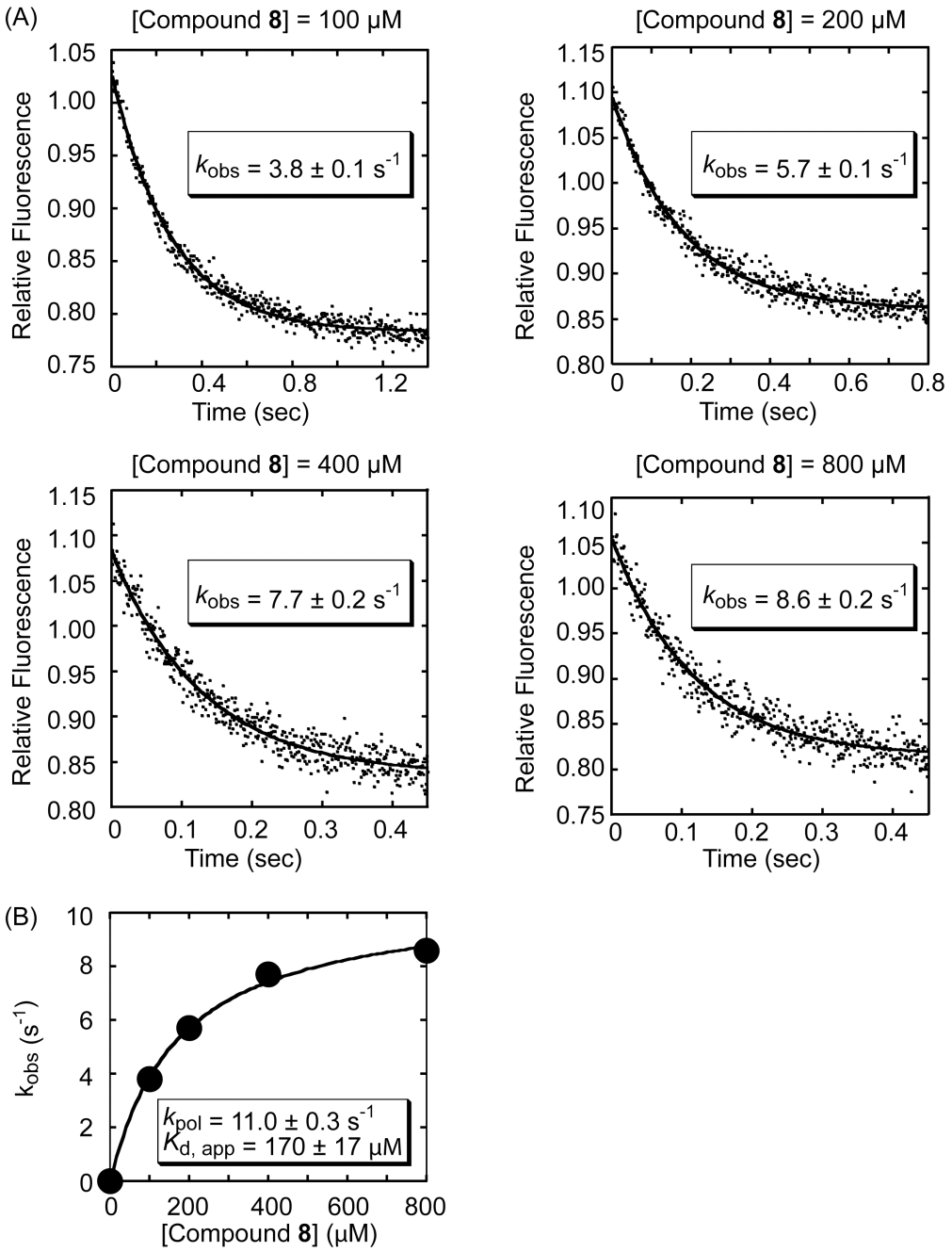

Figure S9. Pre-steady state kinetics of incorporation of **8** into RNA opposite template U by PV RdRP. Panel A: Time courses of incorporation of **8** into RNA by PV RdRP measured with a stopped-flow rapid kinetics apparatus (KinTek Corp.), using an RNA substrate containing the fluorescent reporter 2-aminopurine (*Proc. Natl. Acad. Sci. U.S.A.* **2007,** *104* (11), 4267-4272). Four concentrations of **8** were examined: 100, 200, 400 and 800 μM. The change in fluorescence as a function of time was fit to a single exponential model yielding observed rate constants, k_{obs}. Panel B:. Replot of the observed rate constants as a function of the concentration of **8** and fit to a hyperbolic model yielding estimates of k_{pol} and $K_{d,app}$. Use of the stopped-flow apparatus to measure incorporation kinetics was essentially as previously described (*Proc. Natl. Acad. Sci. U.S.A.* **2007,** *104* (11), 4267-4272).

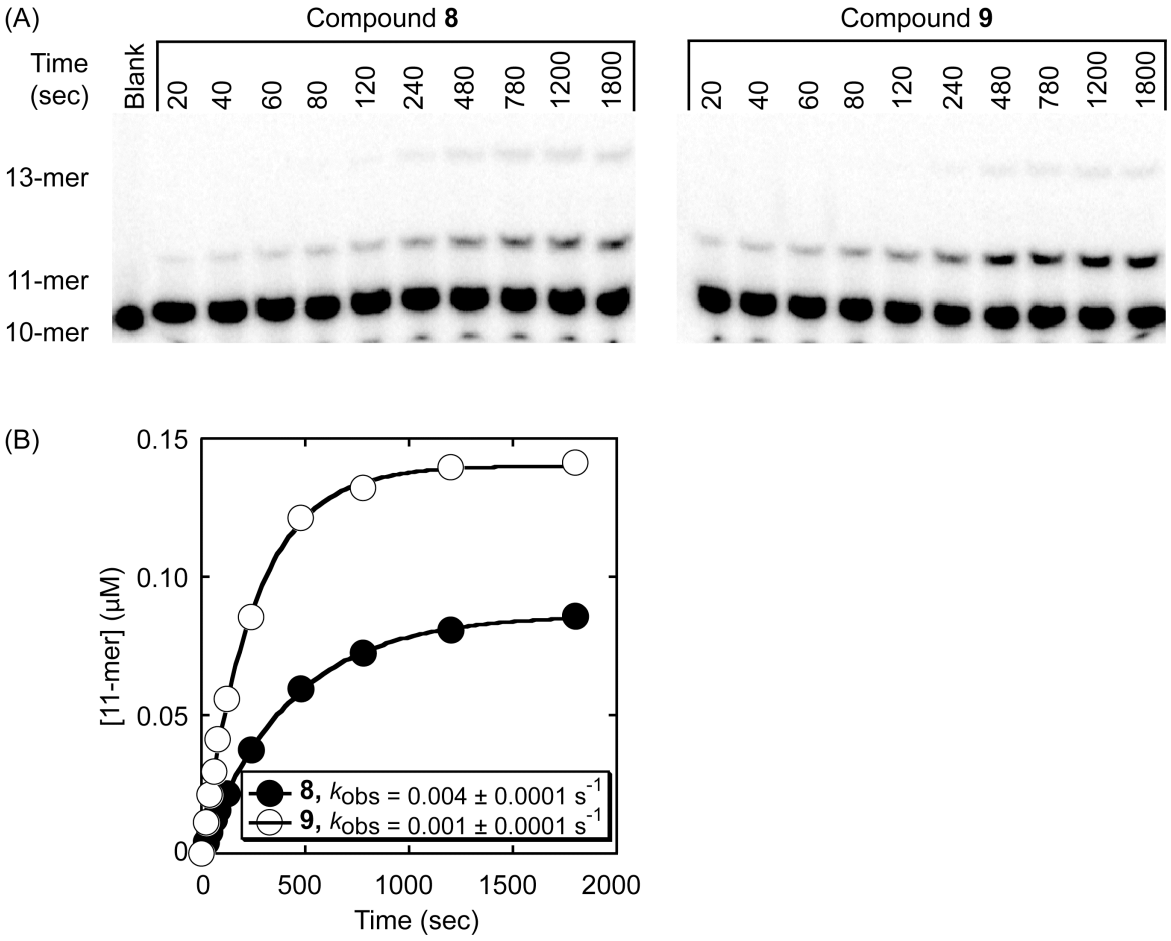

Figure S10. Pre-steady state kinetics of incorporation of compounds **8** and **9** into RNA opposite template C by PV RdRP. Panel A: image of SDS PAGE gel loaded with the extended 10-mer ^{32}P-labeled RNA substrate (illustrated in Figure 3, Panel B) using 2 mM **8** or **9**. The Mg^{2+} concentration was adjusted to maintain 4 mM free Mg^{2+} above the concentration of **8** or **9**. A fifty-fold excess concentration of unlabeled RNA was added at the time of **8** or **9** addition to trap free PV RdRP, thus preventing multiple initiation events by the polymerase. Panel B: Time courses of product formation fitted to a single exponential model. k_{obs} values were further analyzed and refined by simulation to a mechanism that takes into account RdRP-RNA complex dissociation occurring at a rate that competes with the slow rate of **8** or **9** incorporation (data not shown).

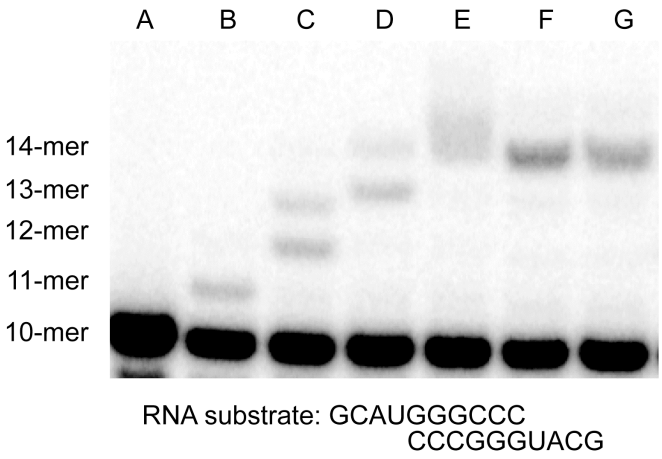

Figure S11.Steady state incorporation of **8**, **9** and natural nucleotides into double-stranded RNA by PV RdRP. Nucleotide incorporation reactions were initiated by addition of PV RDRP. Panel A: no nucleotide; Panel B: ATP; Panel C: ATP, UTP; Panel D: ATP, UTP, GTP; Panel E: ATP, UTP, GTP, CTP; Panel F: **8**, UTP, GTP, CTP; Panel G: **9**, UTP, GTP, CTP.